Supplementary Materials

Optical Properties and Photocatalytic Applications of Two-Dimensional Janus Group-III Monochalcogenides

Aijian Huang,[1] Wenwu Shi,[1,2*] and Zhiguo Wang[1*]

1. School of Electronic Science and Engineering, Center for Public Security Technology, University of Electronic Science and Technology of China, Chengdu, 610054, P.R. China

2. Department of Materials Science and Engineering, North Carolina State University, Raleigh, 27606, United States

*Corresponding author. E-mail: wshi5@ncsu.edu (W. Shi); zgwang@uestc.edu.cn (Z. Wang)

Figure S1 The band structures of (a) InTe (b) In_2SeTe monolayer calculated with PBE functional (left column) and those with PBE+SOC (right column).

Figure S2 The orbital decompositions of the band structures for the (a) GaS (b) GaSe (c) GaTe (d) InSe (e) InTe (f) Ga_2SSe (g) Ga_2STe (h) Ga_2SeTe (i) In_2SeTe monolayers. The vacuum level of X atomic side is set to be zero.

Figure S3 The electrostatic potential for the (a) MX and (b) M_2XY monolayers without dipole correction.

Figure S4 The electrostatic potential for the (a) MX and (b) M_2XY structures with dipole correction. E_{eff} represents the internal effective electric field generated by the intrinsic dipole and $\Delta\Phi$ shows the differences between the vacuum levels at the two surfaces.

Figure S5 Side views of (a) bi- and (b) tri-layered GaS with different stacking configurations. Side views of (c) bi-layered Ga_2SSe with different stacking configurations and (d) tri-layered the energetically stable ABC stacking configuration. The binding energy E_b are shown below the configurations.

Figure S6 The orbital decompositions of the band structures for the (a) bi- and (b) tri-layered GaS and (c) bi- (d) tri-layered Ga_2SSe. The vacuum level of S side is set to be zero.

Figure S7 The real (ε_1) and imaginary (ε_2) parts of the dielectric function for the multilayered (a) GaS and (b) Janus Ga_2SSe structures.

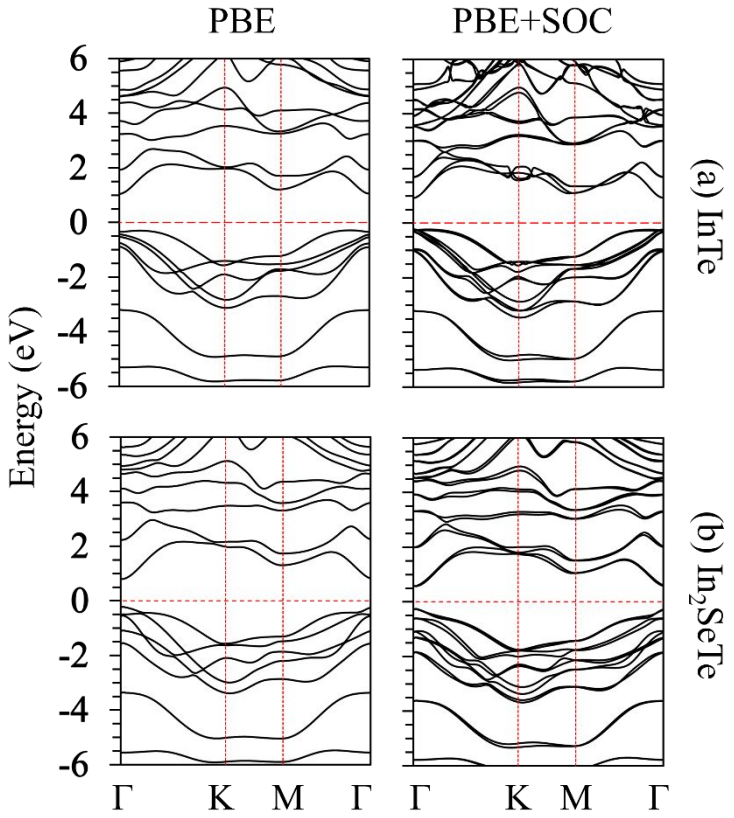

Figure S1 The band structures of (a) InTe (b) In_2SeTe monolayer calculated with PBE functional (left column) and those with PBE+SOC (right column).

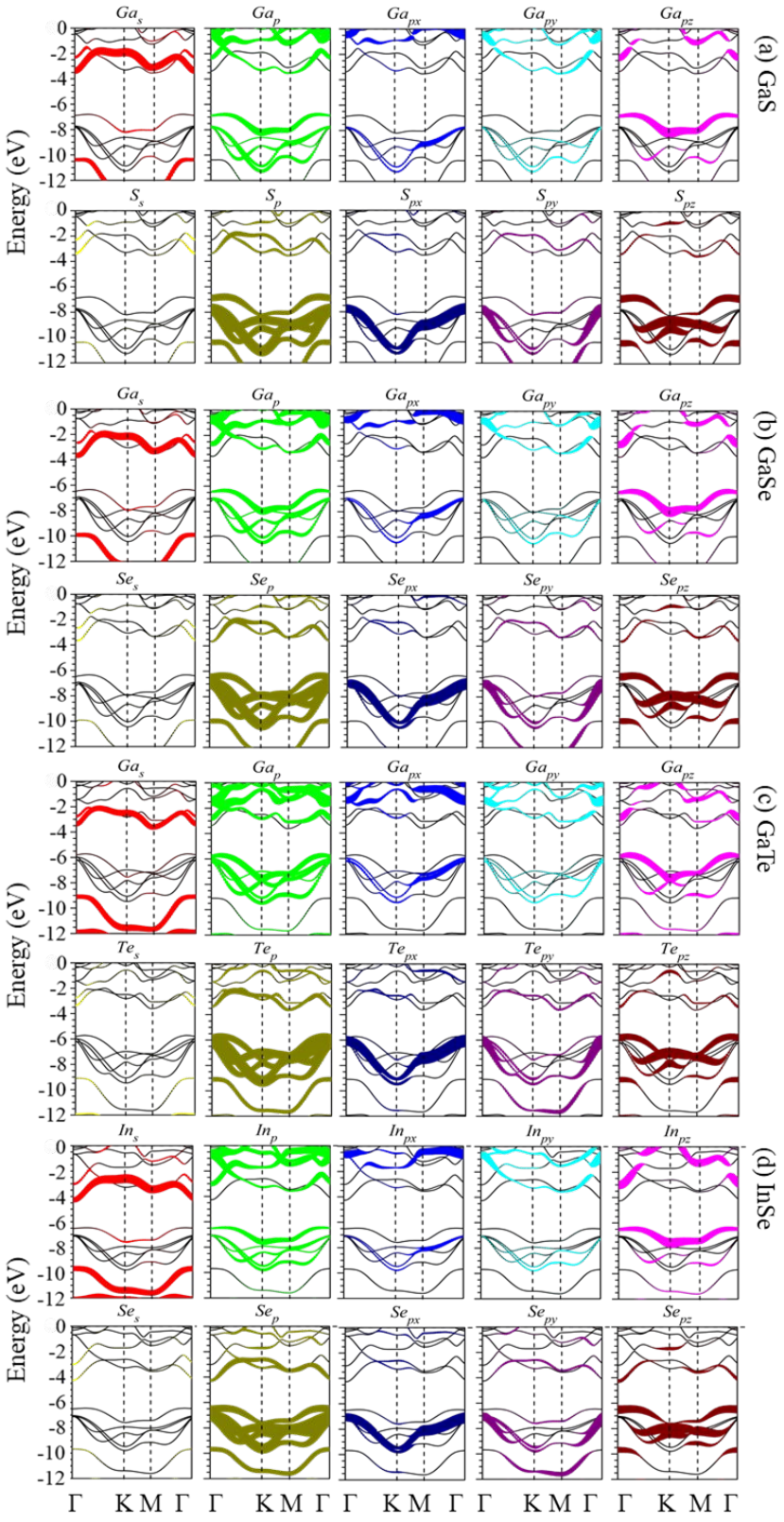
(a) GaS
(b) GaSe
(c) GaTe
(d) InSe
Energy (eV)
Γ K M Γ

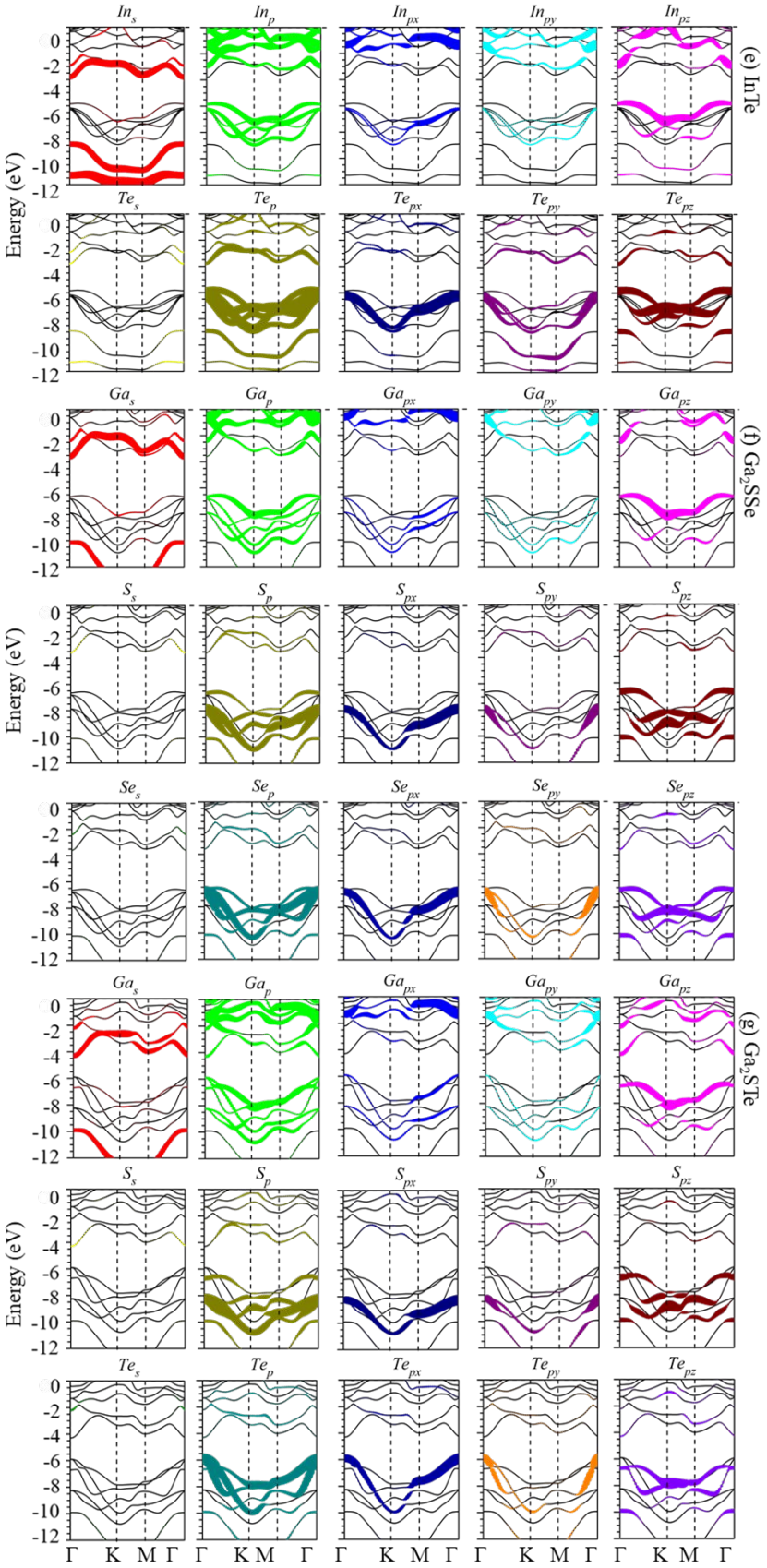
(e) InTe
(f) Ga2SSe
(g) Ga2STe
Energy (eV)
Γ K M Γ

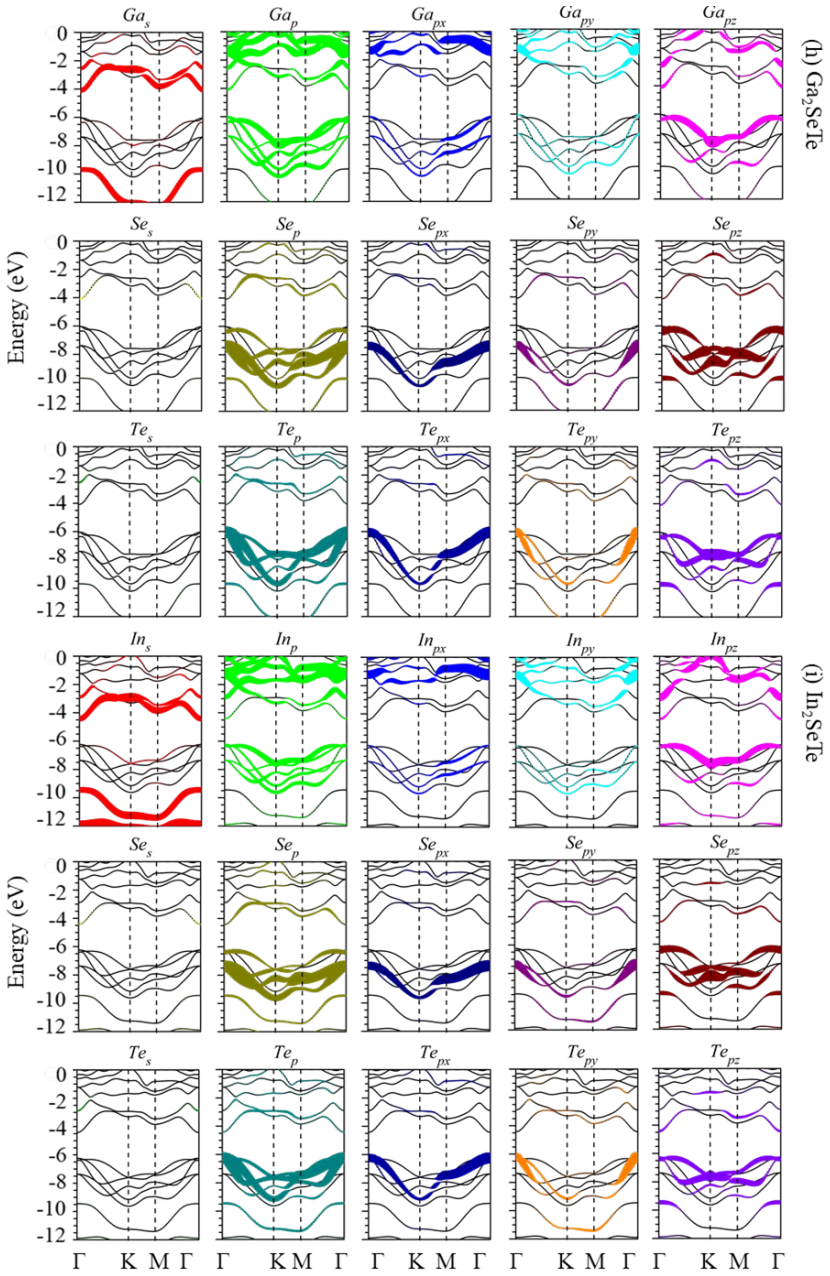

Figure S2 The orbital decompositions of the band structures for the (a) GaS (b) GaSe (c) GaTe (d) InSe (e) InTe (f) Ga_2SSe (g) Ga_2STe (h) Ga_2SeTe (i) In_2SeTe monolayers. The vacuum level of X atomic side is set to be zero.

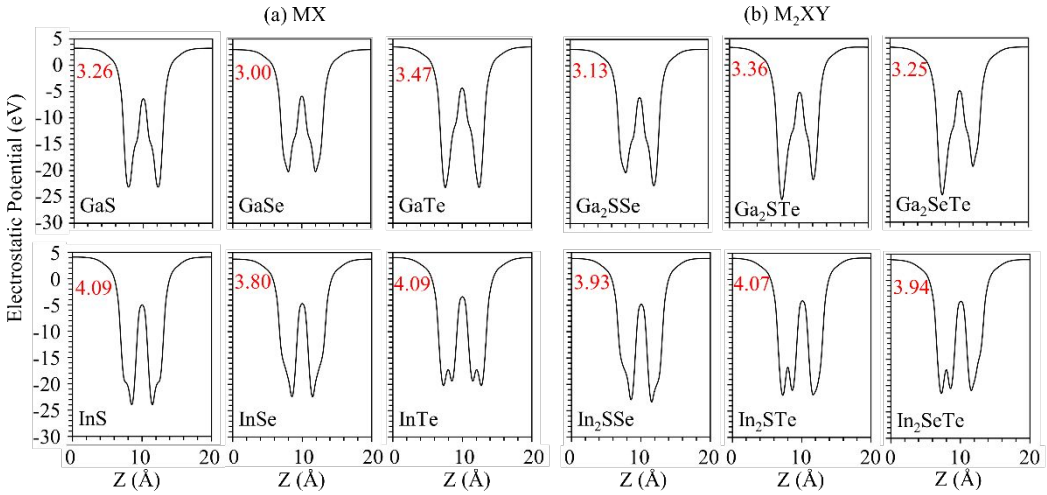

Figure S3 The electrostatic potential for the (a) MX and (b) M_2XY monolayers without dipole correction.

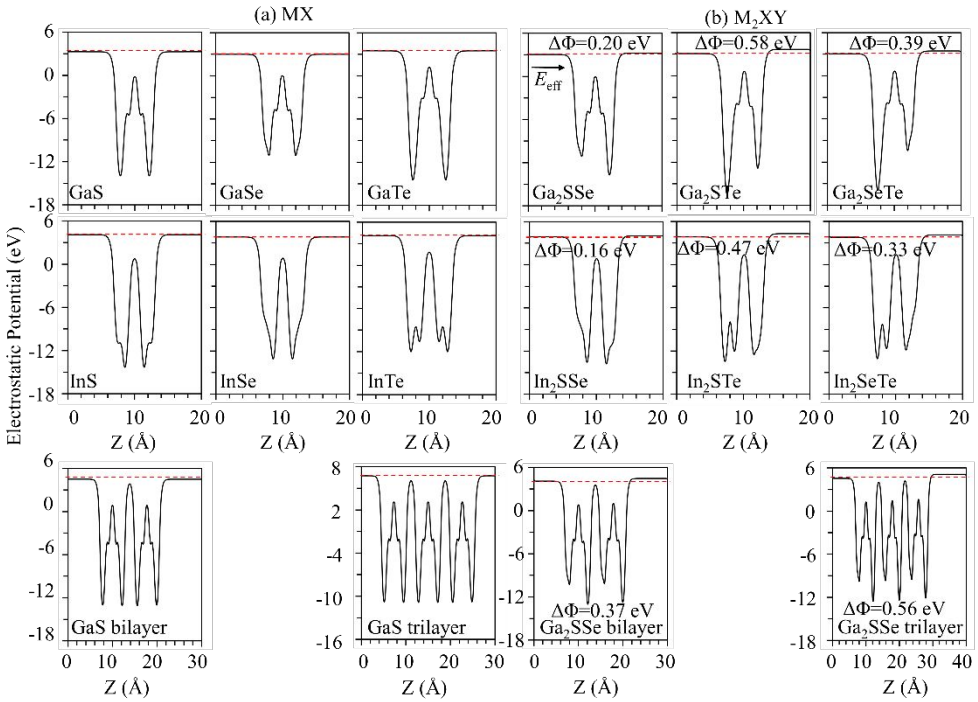

Figure S4 The electrostatic potential for the (a) MX and (b) M_2XY structures with dipole correction. E_{eff} represents the internal effective electric field generated by the intrinsic dipole and ΔΦ shows the differences between the vacuum levels at the two surfaces.

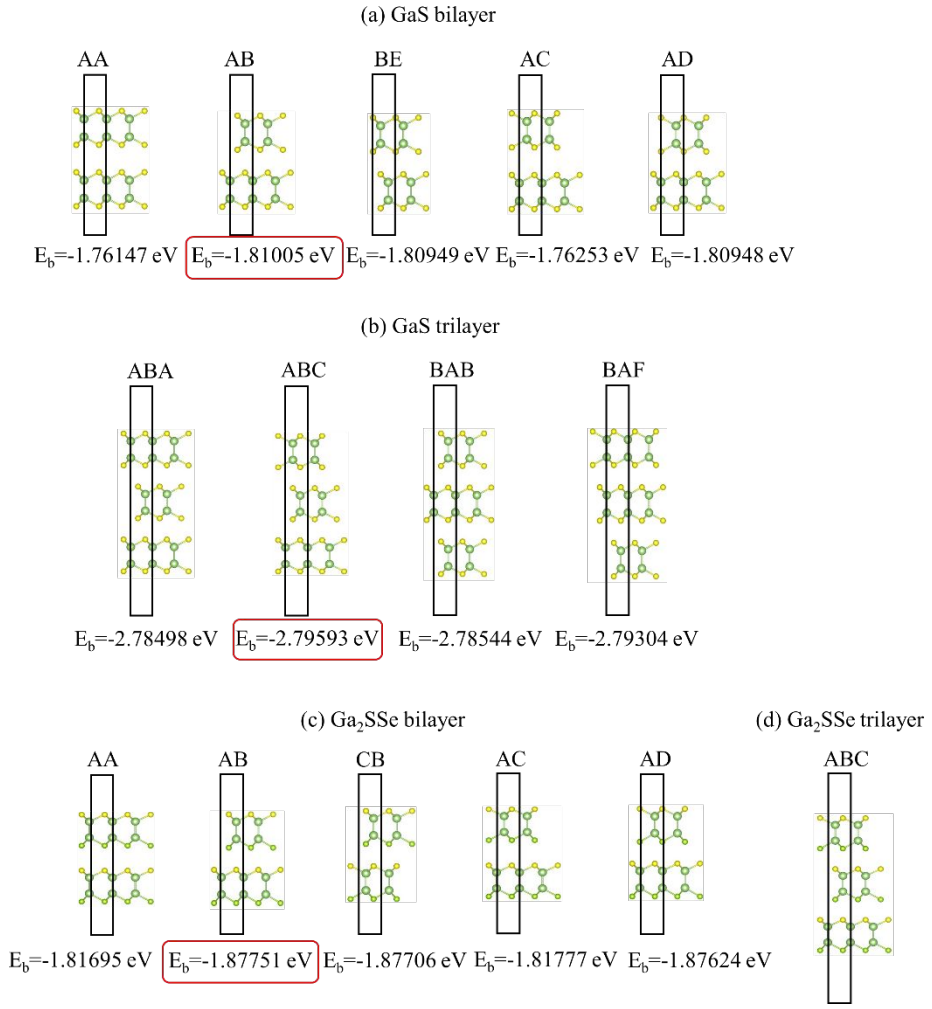

Figure S5 Side views of (a) bi- and (b) tri-layered GaS with different stacking configurations. Side views of (c) bi-layered Ga_2SSe with different stacking configurations and (d) tri-layered the energetically stable ABC stacking configuration. The binding energy E_b are shown below the configurations.

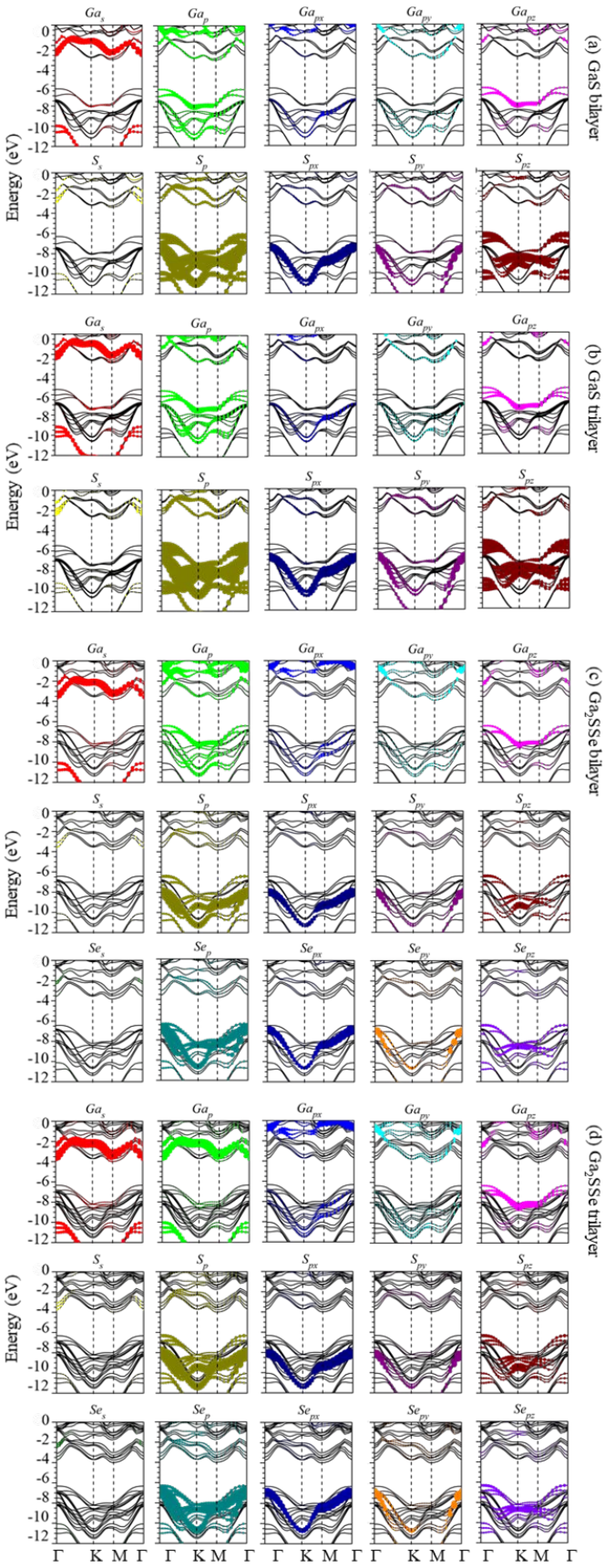

Figure S6 The orbital decompositions of the band structures for the (a) bi- and (b) tri-layered GaS and (c) bi- (d) tri-layered Ga_2SSe. The vacuum level of S side is set to be zero.

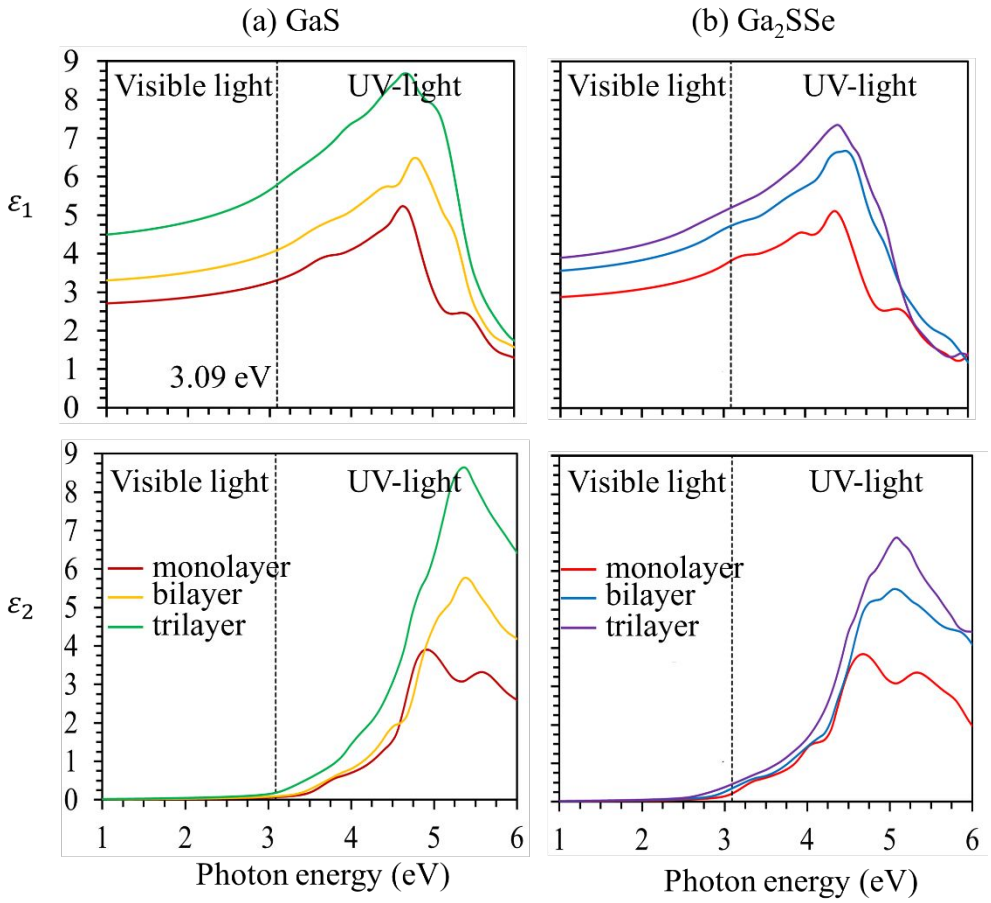

Figure S7 The real (ε_1) and imaginary (ε_2) parts of the dielectric function for the multilayered (a) GaS and (b) Janus Ga_2SSe structures.